Image processing algorithm for detection, quantification and classification of micro defects in wire EDM precision finish cut surfaces

Abhilash P. M.*, D. Chakradhar

Department of Mechanical Engineering, Indian Institute of Technology Palakkad, Kerala, India, 678557

*Corresponding author: abhilashpm184@gmail.com, ORCID ID: 0000-0001-5655-6196

Abstract: The study aims to create an image processing algorithm that categorizes the WEDM finish cut surfaces based on the surface micro defects. The algorithm also detects the defect locations and suggest alternate parameter settings for improving the surface integrity. The proposed automated analysis is more precise, efficient and repeatable than manual inspection. Also, the method can be used for automatic data generation to suggest parameter changes in closed loop systems. During the training phase, mean, standard deviation, and defect area fraction of enhanced binary images are extracted and stored. Training dataset consist of 27 WEDM finish-cut surface images with labels 'coarse', 'average', and 'smooth'. The trained model is capable of categorising any machined surface by detecting the micro defects. If the machined surface image is not classified as smooth image, then alternate input parameter settings will be suggested by the model to minimize the micro defects. This is based on the Euclidean distance between the current image datapoint and the nearest 'smooth' class datapoint.

Keywords: Image processing; machine vision; micro-defects; WEDM; finish-cut

1. Introduction

Non-conventional machining processes possesses several advantages over traditional machining techniques due to the non-contact nature of material removal. Several advancements in the filed of micromanufacturing is achieved by exploiting the negligible cutting forces and stresses involved in non-conventional machining. In the past decade, several researchers have worked towards non-conventional micro manufacturing considering techniques like hybrid wire EDM[1], hybrid EDM[2], and electric discharge wire cutting[3]. Wire electric discharge machining is a variant of electric discharge machining which uses controlled and repetitive

This is a peer-reviewed, accepted author manuscript of the following article: P. M., A., & Chakradhar, D. (2021). Image processing algorithm for detection, quantification and classification of microdefects in wire electric discharge machined precision finish cut surfaces. Journal of Micromanufacturing. https://doi.org/10.1177/25165984211015410

spark erosions for material removal. The process is reported to have immense potential in manufacturing micro components, and can cut complicated geometries with excellent surface finish.[4] The process is capable of achieving a surface finish of 0.4 to 0.8 μm using trim cut strategy.[5,6] Due to this, researchers have attempted to use wire-EDM process as a finishing operation with near zero defects for additive manufactured parts.[7] It is proven that the surface integrity improves considerably by altering the discharge energy and stability of the process.[8-10] During the wire EDM of micro components with high surface finish, one of the main concerns is regarding the presence of micro defects in the form of micro pits, micro globules or micro cracks. These defects can cause the component to fail in thermal and load bearing applications.[11] Several offline models are developed to improve the machining stability of wire EDM process[12-14]. However, in this context, machine vision based automatic inspection techniques are extremely relevant for programmed identification of surface defects.

Katz et al.[15] developed a feedback image processing system for automatic inspection of precision finished surfaces. The system used a vision system to compare a CAD image and actual image and the differences were reported. Image processing techniques were used to detect the defects. Quinsat et al.[16] developed an in-situ inspection system to compare the machined parts with the CAD model using a vison system. Based on the correlation between the two, machining optimization is performed to minimize the differences. Chen et al.[17] proposed an image processing technique for automatic damage detection of finished ceramic surfaces through grinding operation. Raw image is processed through noise cancellation, contrast adjustments and segmentation. Defect classification was also performed based on shape and texture. Martínez et al.[18,19] developed an image fusion technique to identify the defects irrespective of their orientation with respect to the surface texture formed by finish operation. Image processing techniques were used in various lighting conditions and the results were verified. Tsai and Molina[20] developed a vision-based defect detection system in machined

components with circular tool marks. They introduced arc shaped structural elements in polar coordinates for defect identification. Steiner and Katz[21] framed an image processing technique to inspect and measure the porosity defects on machined components. Different algorithms were proposed for detection of edge pores and normal surface pores. Swillo and Perzyk [22,23] developed a machine vision system for automatic detection of casting defects after machining. The image processing algorithm uses edge detection operation based on modified Laplacian filter. Liao et al.[24] developed a defect feature identification and classification model for machined surfaces. Illumination direction was emphasised in this work. Huang et al.[25] developed a deep learning-based defect detection model in a smart factory environment. A convolutional neural network (CNN) learning algorithm is proposed for defect detection. Frayman et al.[26] proposed a defect detection method based on computer vison for identification of surface defects in aluminum die cast components. A genetic algorithm (GA) optimizes the image processing parameters to extract right number of features. Manish et al.[27] developed an image processing inspection technique for defect detection during grinding operation. Canny Edge detection algorithm is used for defect edge identification, were dark patches indicated defects and fine region were indicated by closely spaced edge lines. Li et al.[28] proposed an algorithm to detect defects from scanning electron microscope (SEM) images. The computer vision-based approach automates the inspection process using CNN classification algorithm.

The industrial demands are pushing the precision finish machining processes towards zero surface defect tolerance approach. From the literature study it was found that the existing studies have not yet proposed a closed loop system wherein not only the machined surfaces are classified based on defects, but also better parameters are suggested for defect free finish. In this regard, this paper introduces an image processing-based surface classification technique to categorize machined Inconel 718 surfaces. Moreover, the algorithm automatically detects the

defect features and suggests alternate parameter settings to improve the machined surface quality.

2. Materials and Equipments

2.1 Material selection

Inconel 718 superalloy is considered as the workpiece material for this study to demonstrate the capabilities of the algorithm. The chemical composition and mechanical properties of Inconel 718 are given in Table 1 and Table 2. Zinc coated hard brass wire of 0.25 mm diameter is considered as the wire material due to its higher performance in comparison with the uncoated wire electrodes.

Table 1. Chemical composition of Inconel 718 [29]

Element	Ni	Fe	Cr	Nb	C	Al	Ti	Mo
Weight (%)	Balancing	18.5	19	5.1	0.04	0.5	0.9	3

Table 2. Mechanical properties of Inconel 718 [30]

Property	Value
Density	8.19 g/cm^3
Melting point	1260 – 1336^o C
Specific heat	435 J/kg K
Coefficient of thermal expansion	13 μm /m K
Thermal conductivity	11.4 W/m K
Ultimate tensile strength	1240 MPa

2.2 Experimental setup

Electronica ECOCUT wire EDM machine is used to machine Inconel 718 material. The wire EDM setup is shown in Fig. 1. De-ionized water is used as the dielectric fluid. Zeiss Gemnisem 300 field emission scanning electron microscope is used to image the machined surfaces. The machined surfaces are imaged in 1500X magnification using a field electron scanning electron microscope (FESEM) for analysis. Standard image resolution is maintained at 768 x 1024. However, if the pixels of the microstructural image are more or less, ‘image

resize' function in MATLAB is used to bring it to the standard acceptable size for the algorithm to work. Accuracy of defect identification and detection is thus preserved in all cases irrespective of image pixel size. Table 3 shows the parameter settings and levels. Lower discharge energy settings were opted to get a micro finished surface. All the considered input parameters, namely T_{ON}, T_{OFF}, and servo voltage has an effect on surface defect. The different input levels are chosen intentionally to create surfaces which ranges from extremely smooth to extremely coarse. Thus, the training images contains different ranges of defect coverages from < 10 % to > 90 %. The dataset is thus a true representation of all types of electric discharge machined surfaces. Accuracy of the defect detection and classification will be similar even when different input levels are considered. This is verified by conducting confirmation experiments. The parameters, levels and ranges were selected based on pilot experiments, information from wire EDM manual, and literature survey. Emphasis was given to cover different regimes of machined surface quality. In the current study, other parameter settings are maintained constant due the wire EDM constraints and lesser effect on machined surface quality. The details are given in Table 4.

Fig. 1 Wire EDM equipment

Table 3 Details of parameter settings

Factors	Level 1	Level 2	Level 3
Pulse on time (T_{ON}) (μs)	5	10	15
Pulse off time (T_{OFF}) (μs)	10	15	20
Servo Voltage (V)	15	20	25

Table 4 Constant parameters

Parameter	Value
Wire electrode diameter	0.25 mm
Discharge current	11 A
Wire feed rate	3 m/min
Discharge voltage	12 V
Flushing pressure	1.96 bar
Wire Tension	10 N
Dielectric fluid	Deionized water

3. Image processing method

The visual defect identification system includes the following subcategories: image acquisition, image pre-processing and enhancement, feature extraction and defect representation, and human computer interaction. First the machined surface image is captured through a microscope. Pre-processing of the raw image is done by grey scale conversion, contrast enhancement and histogram equalisation. Further, under image enhancement, the pre-processed images are converted to binary images based on a threshold. The image is then filled to reduce noise gaps. As the final step in image enhancement, the image is smoothed using a structural disk element. Once the image is enhanced through the aforementioned steps, the defect identification is convenient. The defect is identified to exist around the centroid of the enhanced image features and the defect area is marked in rectangular box. A classification model is trained based on the mean, standard deviation and defect area fraction of the enhanced image. The schematic diagram of the proposed machine vision system is shown in Fig. 2. The process involved in defect feature identification based on image processing is given in Fig. 3.

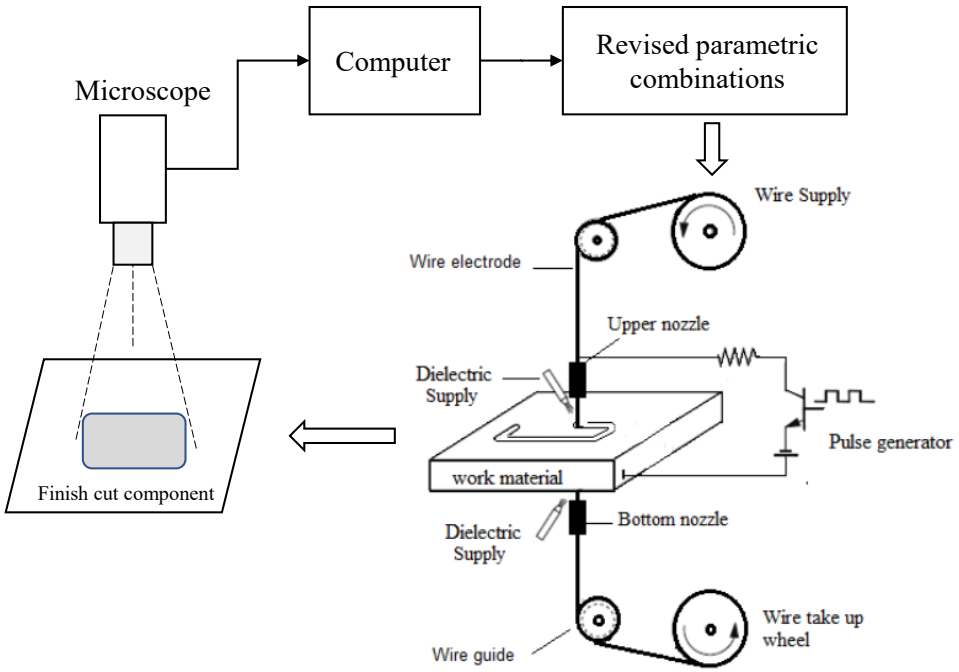

Fig. 2 Schematic diagram of wire electric discharge machine vision system

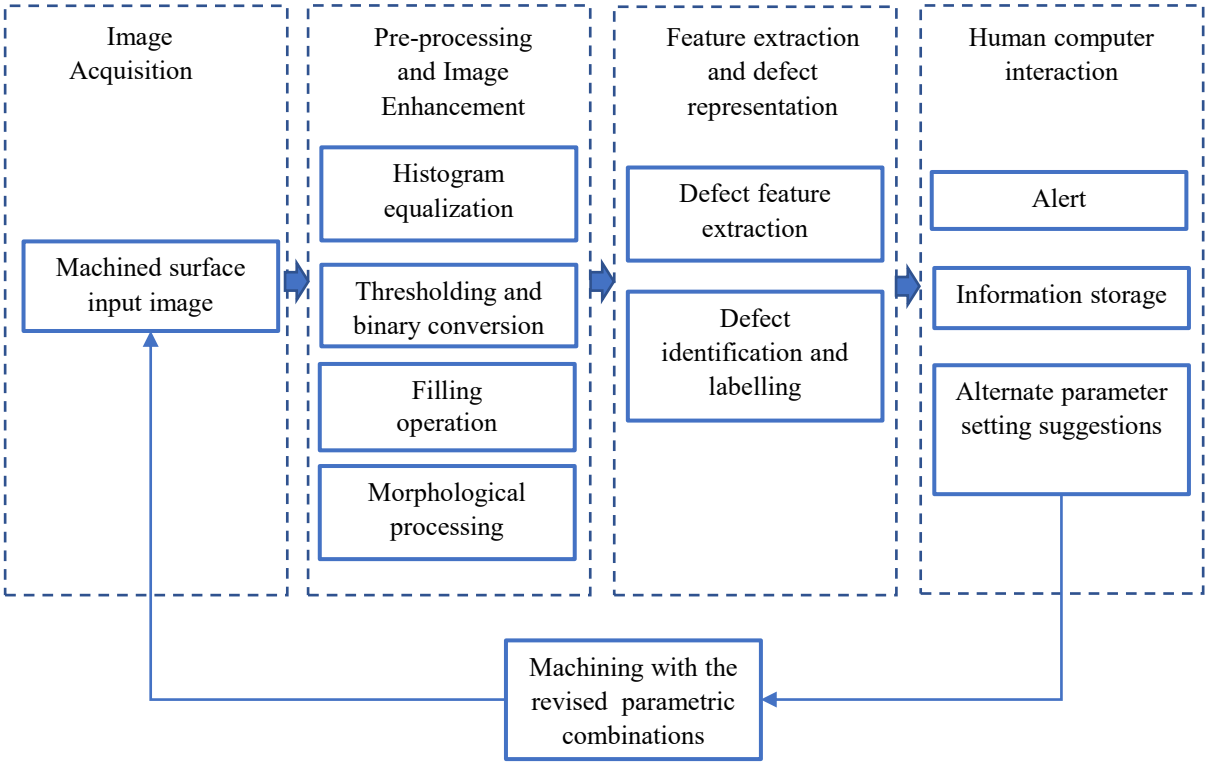

Fig. 3. Image processing steps involved in machined surface defect feature detection

3.1 Image pre-processing and enhancement

Image acquisition involves capturing the machined surface image for defect analysis. The machined samples are observed under a high magnification microscope (in this case, a SEM), to capture the raw image. The captured raw image is pre-processed by performing contrast adjustment, and histogram equalization operations. The histogram equalization distributes the output image intensities uniformly as shown in Fig. 4. The image transformations after the pre-processing steps are shown in Fig. 5. The step aims to supress unwanted noises and to make the digital image more uniform and suitable for further processing. It could be observed that the surface defects are much clearly visible in Fig. 5 (c) compared to Fig. 5 (a).

The defects on an electric discharge machined surface are globule shaped irregularities which are caused by re-solidification of molten metal during the spark erosion process. The number and extend of these defects are the basis for categorising the machined surfaces into coarse or smooth. To distinguish these defect features from the base surface, the following image enhancement operations were conducted; binary conversion, gap filling, and morphological operation as shown in Fig. 6.

Binary conversion: The grey scale image is converted to binary image by setting a threshold value by this operator. The operator converts all pixel values above a particular threshold to 1 and others to zero. The result of operation is showed in Fig. 6 (b).

Filling operation: The smaller holes are filled by this operation. The holes are the white pixels surrounded by the black pixels. The result of filling operation is showed in Fig. 6(c).

Morphological operation: The image erosion operation smoothens the image by flat structuring element, in this case a disk element of specified radius. The image is eroded from region boundaries in the shape of the disk structuring element of radius 15 pixels. The eroded image is shown in Fig. 6 (d).

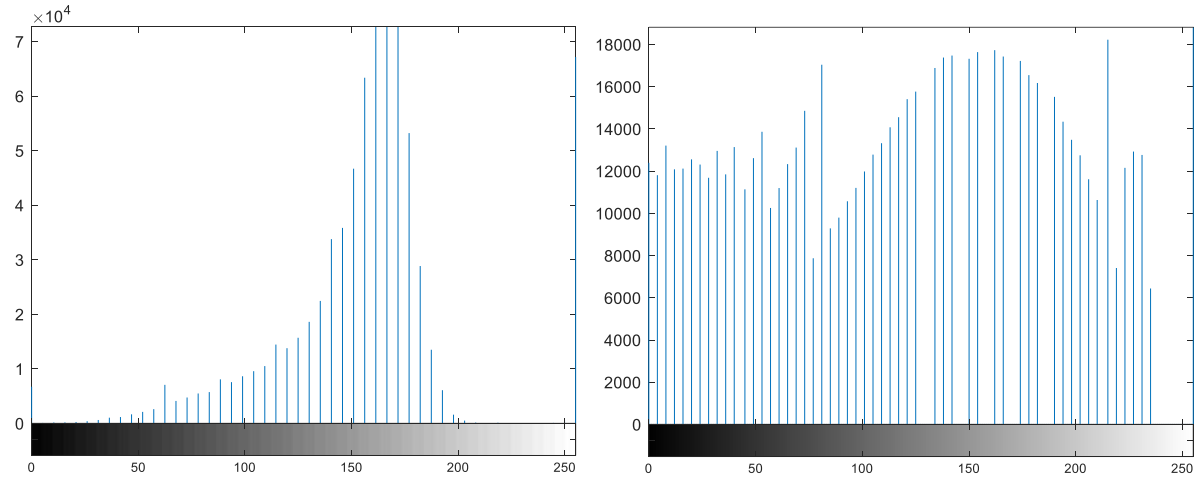

Fig. 4 (a) Histogram of raw image (b) Histogram of equalised image

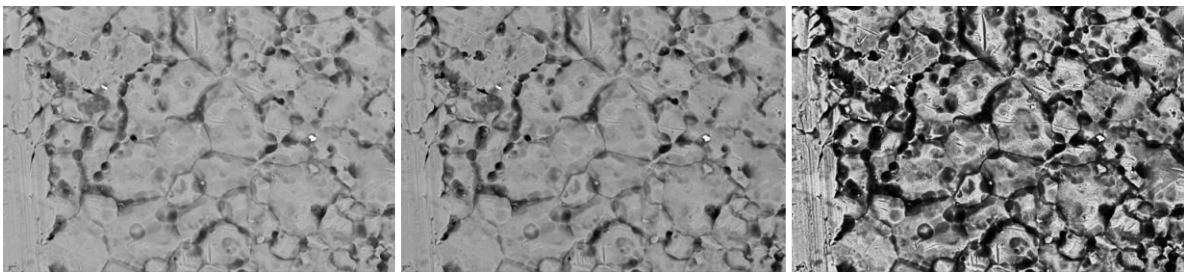

Fig. 5 Image pre-processing steps (a) Raw image (b) Contrast adjusted image (c) Histogram equalised image

3.2 Defect feature detection

Steps in defect detection and marking from the enhanced image:

Step 1: Identifying all connected white pixels in the 2D binary image. Pixels of separate regions are numbered differently. In Fig. 7 (a), a separate colour is assigned for each region. A comparison with the original image shows that all the surface defects are detected as different regions. Also, the number of such defect regions is stored.

Step 2: Area and bounding rectangle of each region are calculated. Bounding rectangle is the smallest rectangle that can enclose the region completely. This is for displaying the feature locations in the original image as shown in Fig. 7 (b). The area calculation disregards the rectangular area, but considers the actual fitted boundary for calculations. This is performed by area function in MATLAB which calculates the area by considering the number of white pixels

in the enhanced binary image. The percentage of total pixel area covered by the defect feature is calculated by the formula

$$\%\ Surface\ defects = \left(\frac{Total\ area\ of\ defect\ features}{Total\ area\ of\ machined\ surface\ image}\right) x\ 100$$

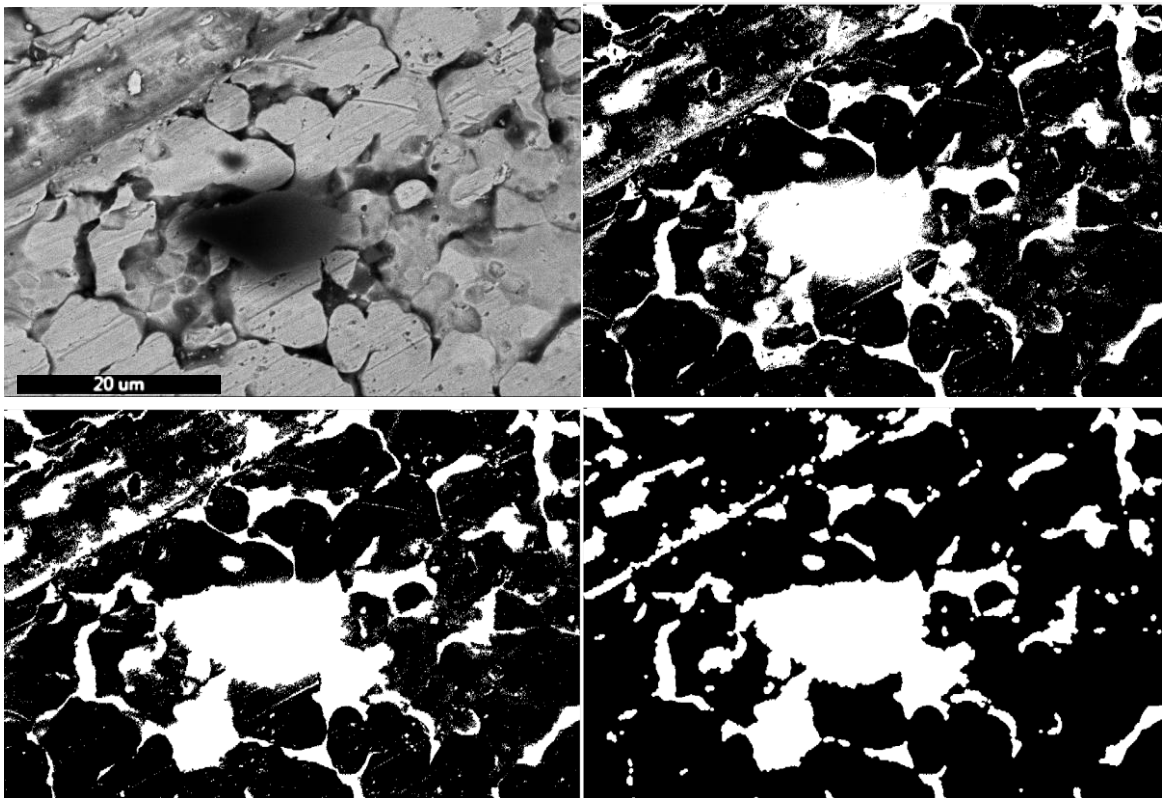

Fig. 6 Image enhancement steps for a coarse surface (a) pre-processed image (b) binary operator (c) filling operation (d) morphological operator (extracted defect profile)

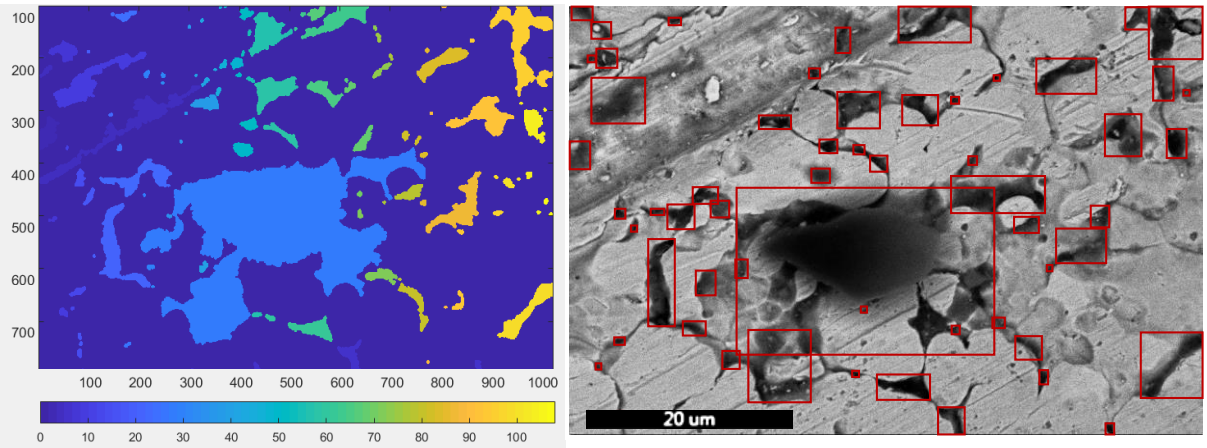

Fig. 7 Defect feature detection from enhanced binary image (a) representation of defect regions (b) defect features are identified and labelled

Step 3: Mean, standard deviation and defect area fraction of the enhanced binary image is calculated and stored. The proof of concept for image classification from the statistical measures is already investigated and established by Kumar and Gupta.[31] If the pixel matrix of enhanced binary image I, is made of n pixels, the standard deviation is given by

$$SD = \sqrt{\frac{1}{n-1}\sum_{i=1}^{n}|I_i - \mu|^2}\,,$$

where μ is the mean value of the pixel matrix I, given by

$$\mu = \frac{1}{n}\sum_{i=1}^{n} I_i$$

Defect area fraction is the normalised value of the area of white region (defects) by the total binary image area.

3.3 Surface classification

The training data set for machined surface classification consists of 27 machined surface images with their class labels. All the images are categorised into 3 labels based on the roughness values as given in Table 5. The features like mean, standard deviation and damage area fraction of pixel matrix were extracted. Let the training dataset be

$$P_t = (m_t, sd_t, a_t) \quad \text{where t = 1, 2 …, 27}$$

where m_t, sd_t, and a_t are the mean, standard deviation, and damage area fraction of t^{th} training datapoint. Whenever a new machined surface image is fed to the model, the model performs feature extraction procedure to find the mean and standard deviation of the input image. Let the input image datapoint be

$$P_i = (m_i, sd_i, a_i)$$

where m_i, sd_i, and a_i are the mean, standard deviation, and damage area fraction of i^{th} input datapoint. The K nearest neighbour (K-NN) classification algorithm finds the nearest training

set data point to this point by least Euclidean distance between the training and input datapoints. K parameter value is considered as 1 in this case. The Euclidean distance is calculated by the following formula

$$dist\ (P_t - P_i) = \sqrt{(m_i - m_t)^2 + (sd_i - sd_t)^2 + (a_i - a_t)^2}$$

The flowchart of k-NN classification algorithm is given in the Fig. 8. The classification model is schematically represented in Fig. 9.

Table 5 Surface classes and names

Classes	Surface type	Criteria
Class 1	Smooth	Ra < 1µm
Class 2	Average	Ra = 1 µm to 2.5 µm
Class 3	Coarse	Ra > 2.5 µm

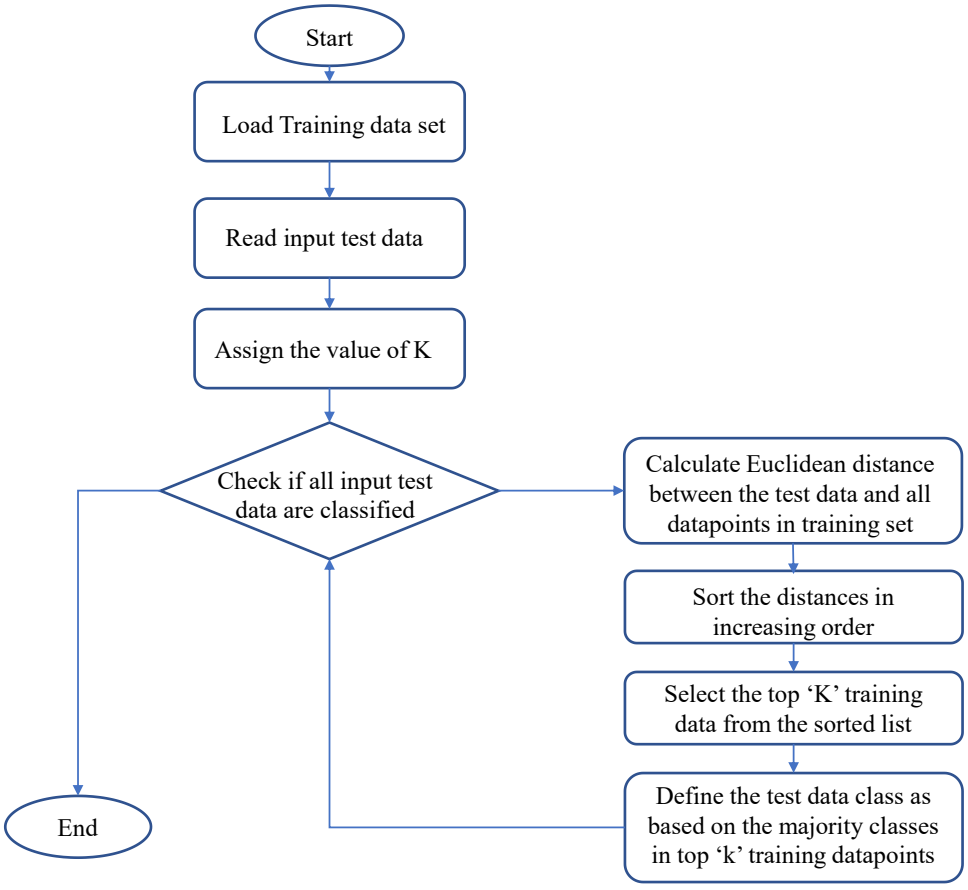

Fig. 8 K-NN classification flowchart

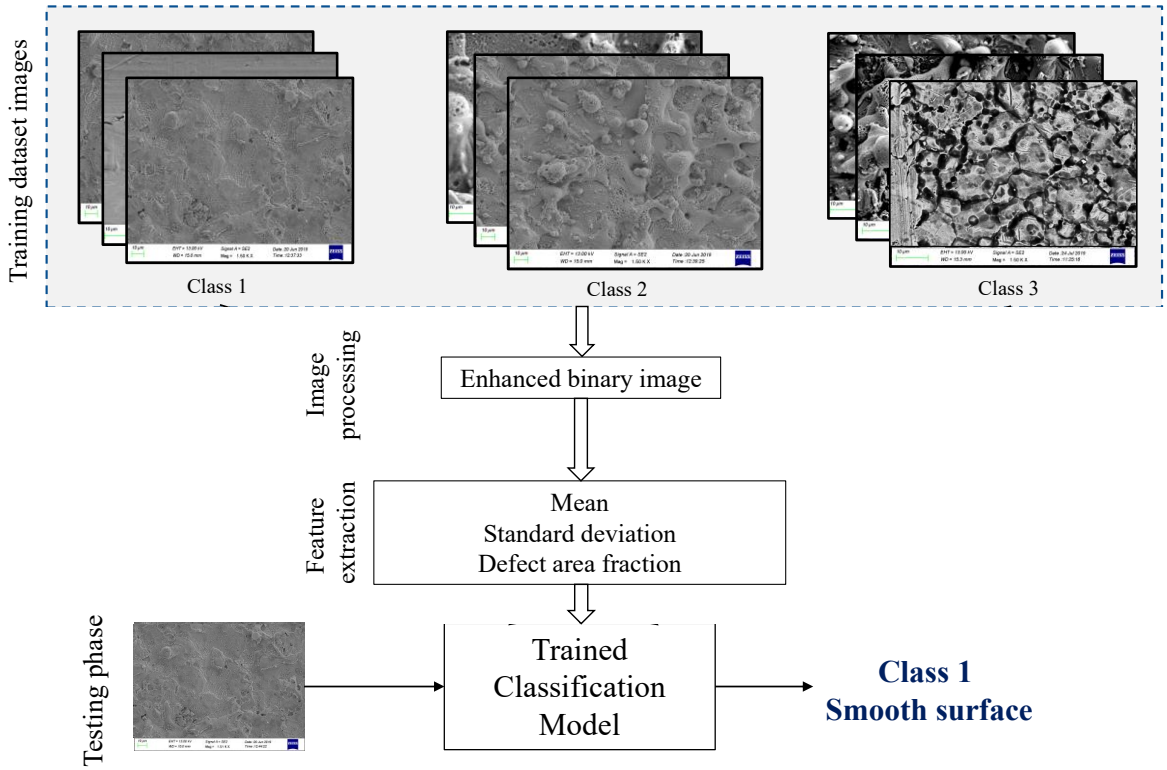

Fig. 9 Machined surface classification model

4. Results and Discussion

Twenty-seven images belonging to three different categories were selected to train the algorithm. The various stages of micro defect detection are shown in Fig. 10. It could be observed that the surface defects in linear form, negative defects (pits or craters) or positive defects (globules) could be identified by the algorithm. The total area covered by the defects varies in each case. In the first case, the surface is smooth in most areas except a linear surface peeling type defect. Therefore, the area covered by the defect is the minimum of the three cases at 10.02%. Second case shows the surface covered by micro pores. The spread of the defects is greater compared to the previous case and the area covered by defects are 20.8%. In the final case, most of the surface is covered by micro globules. 73.29 % area is covered by defects.

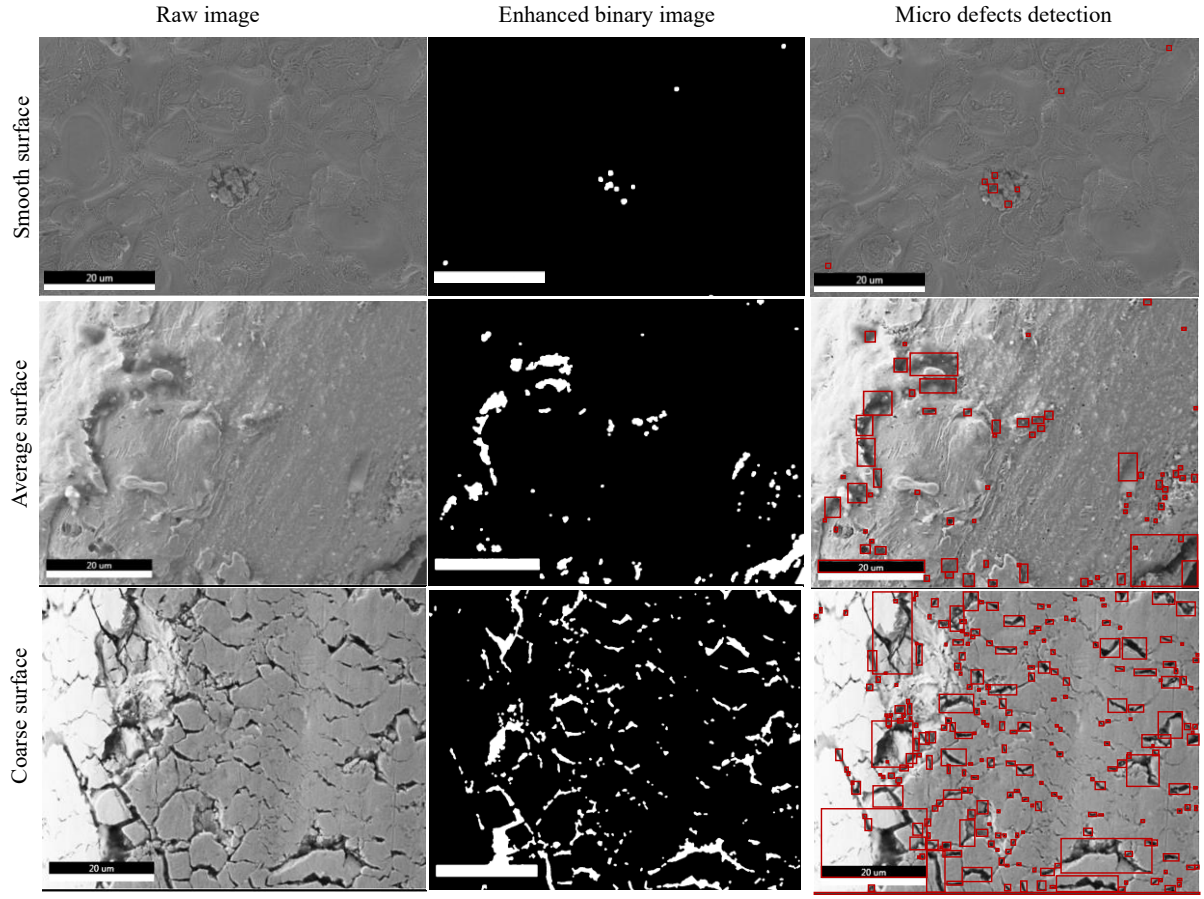

Fig. 10 Stages of micro defects detection

The mean, standard deviation, and defect area fraction of the 27-training dataset is extracted from the enhanced binary images. The details are shown in Table 6. And the accuracy of the proposed algorithm in classifying the surfaces based on defects are represented through a confusion matrix given in Fig. 11. The algorithm is observed to have an accuracy of 96.3 % in classifying the surfaces based on the micro defects. As mentioned in previous section, the criteria for class label for training images is the measured surface roughness values.

The extracted features of training set are plotted in Fig. 12. When a new test image is fed to the algorithm, the image is pre-processed and enhanced for feature extraction. The features extracted from the test image are mean and standard deviation of the enhanced binary image and the defect area fraction. The training data already has the extracted features of 27 images along with its corresponding class. The classification algorithm is responsible for identifying

the nearest training datapoint to the test image data point. Fig. 13 shows the test data point in red, plotted against training data sets. It is clear that the point is nearer to the datapoints plotted in green, which corresponds to coarse images. So, the test image is categorised as 'coarse'.

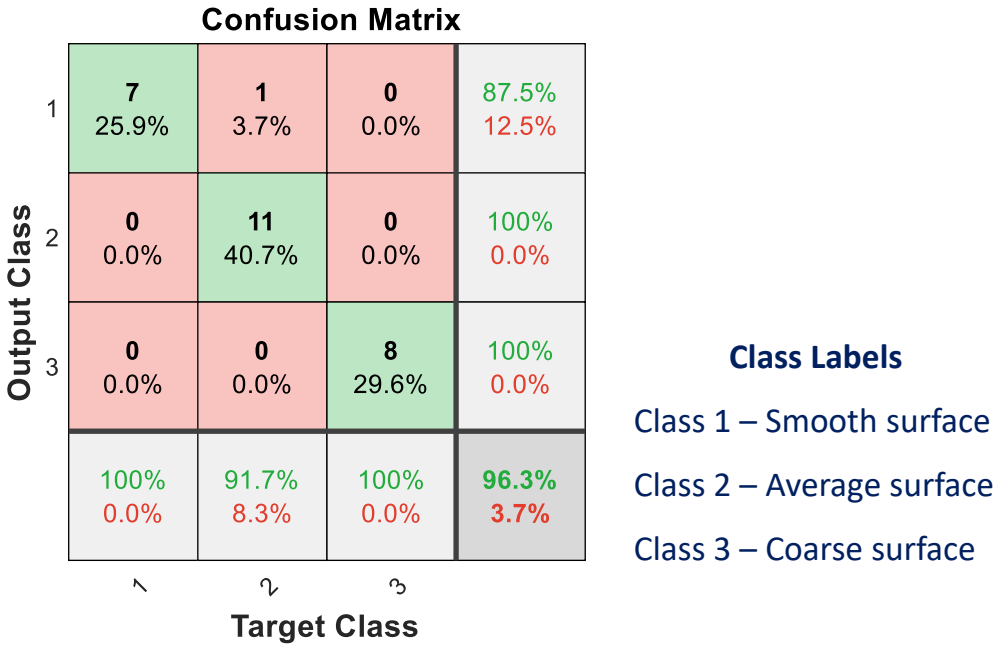

Fig. 11 Confusion matrix to evaluate the classifier performance

Table 6 Features extracted from training images

S. No.	T_{on} (µs)	T_{off} (µs)	SV (V)	Extracted features			Class
				Mean	Standard deviation	Defect area fraction	
1	5	10	15	0.492	0.037	0.508	2
2	5	10	20	0.614	0.025	0.386	2
3	5	10	25	0.631	0.027	0.369	2
4	5	15	15	0.893	0.013	0.107	1
5	5	15	20	0.796	0.043	0.204	2
6	5	15	25	0.9	0.001	0.100	1
7	5	20	15	0.896	0.01	0.104	1
8	5	20	20	0.792	0.053	0.208	2
9	5	20	25	0.9	0.001	0.100	1
10	10	10	15	0.453	0.015	0.547	2
11	10	10	20	0.508	0.023	0.492	2

12	10	10	25	0.302	0.043	0.698	2
13	10	15	15	0.229	0.096	0.771	3
14	10	15	20	0.514	0.044	0.486	2
15	10	15	25	0.774	0.048	0.226	2
16	10	20	15	0.898	0.005	0.102	1
17	10	20	20	0.844	0.04	0.156	1
18	10	20	25	0.899	0.002	0.101	1
19	15	10	15	0.009	0.085	0.991	3
20	15	10	20	0.031	0.128	0.969	3
21	15	10	25	0.18	0.092	0.820	3
22	15	15	15	0.047	0.141	0.953	3
23	15	15	20	0.117	0.096	0.883	3
24	15	15	25	0.187	0.1	0.813	3
25	15	20	15	0.267	0.055	0.733	3
26	15	20	20	0.378	0.027	0.622	2
27	15	20	25	0.483	0.018	0.517	2

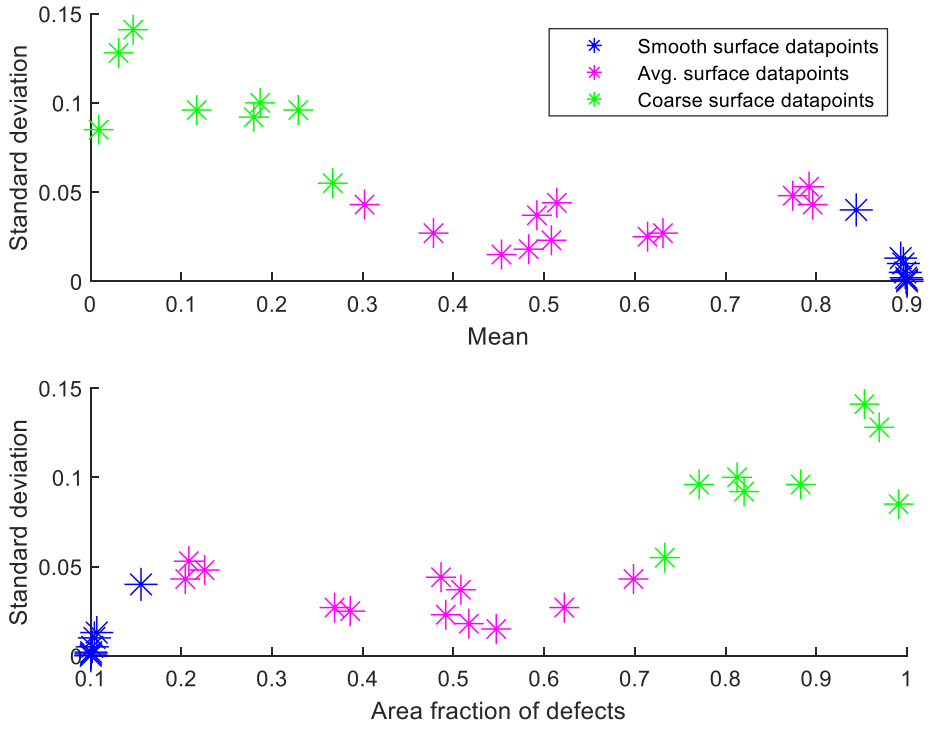

Fig. 12 Plotting different categories of machined surfaces based on extracted features (a) Mean vs. standard deviation (b) Area fraction vs. standard deviation

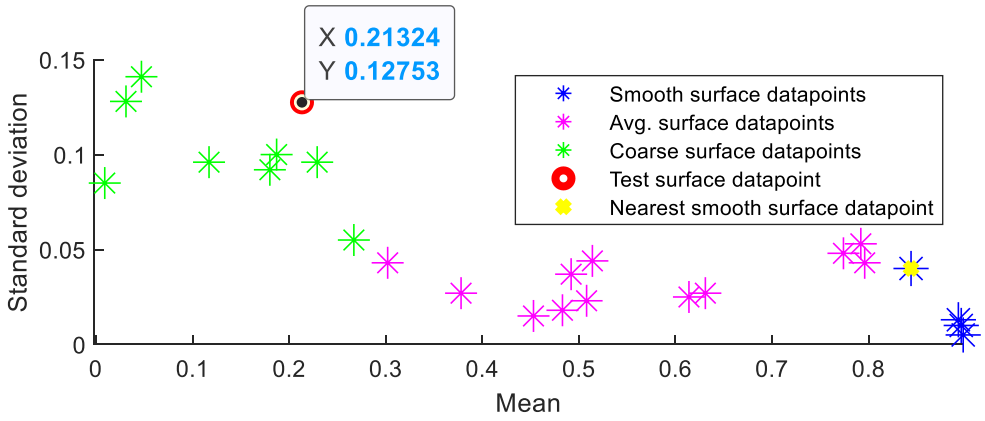

Fig. 13 Locating the test image datapoint classified as 'coarse surface' based on Euclidean distance

4.1 Confirmation experiments

Nine confirmation experiments were conducted to test the performance of the algorithm in real world machining situations. Table 7 shows the details of the features extracted and classification. Once an input test image is received, the algorithm displays the following information about the surface, as shown in Fig. 14. (a) Defect locations (b) Number of micro-defects (c) Surface category. Fig. 15 shows the micro defect detection, feature extraction and surface classification for three different test images belonging to confirmation experiments.

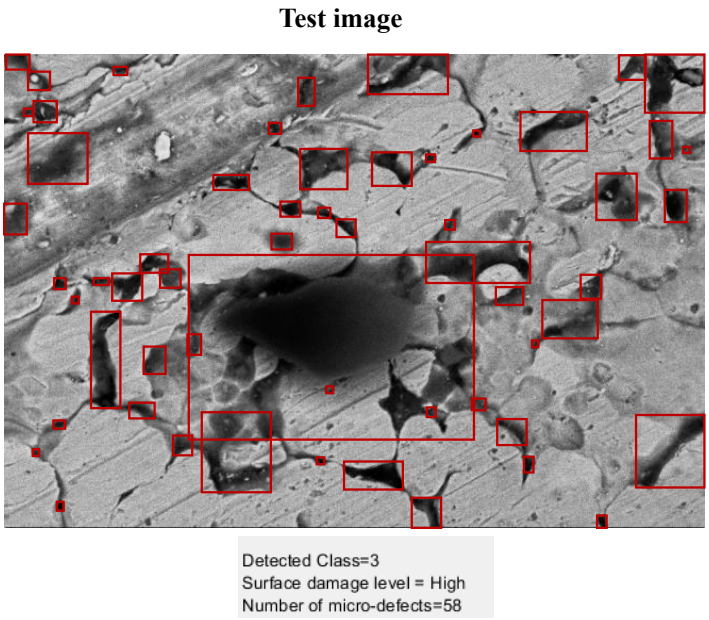

Fig. 14 Defect locations and surface category getting displayed

Table 7 Confirmation experiments

S. No.	T_{on} (µs)	T_{off} (µs)	SV (V)	Extracted features			Class
				Mean	Standard deviation	Defect area fraction	
1	6	12	24	0.893	0.013	0.118	1
2	5	18	21	0.884	0.016	0.137	1
3	11	19	17	0.673	0.043	0.341	2
4	14	11	16	0.217	0.121	0.861	3
5	15	12	15	0.013	0.085	0.989	3
6	17	10	15	0.161	0.065	0.784	3
7	15	19	22	0.472	0.027	0.482	2
8	13	18	25	0.511	0.038	0.531	2
9	12	20	21	0.688	0.029	0.419	2

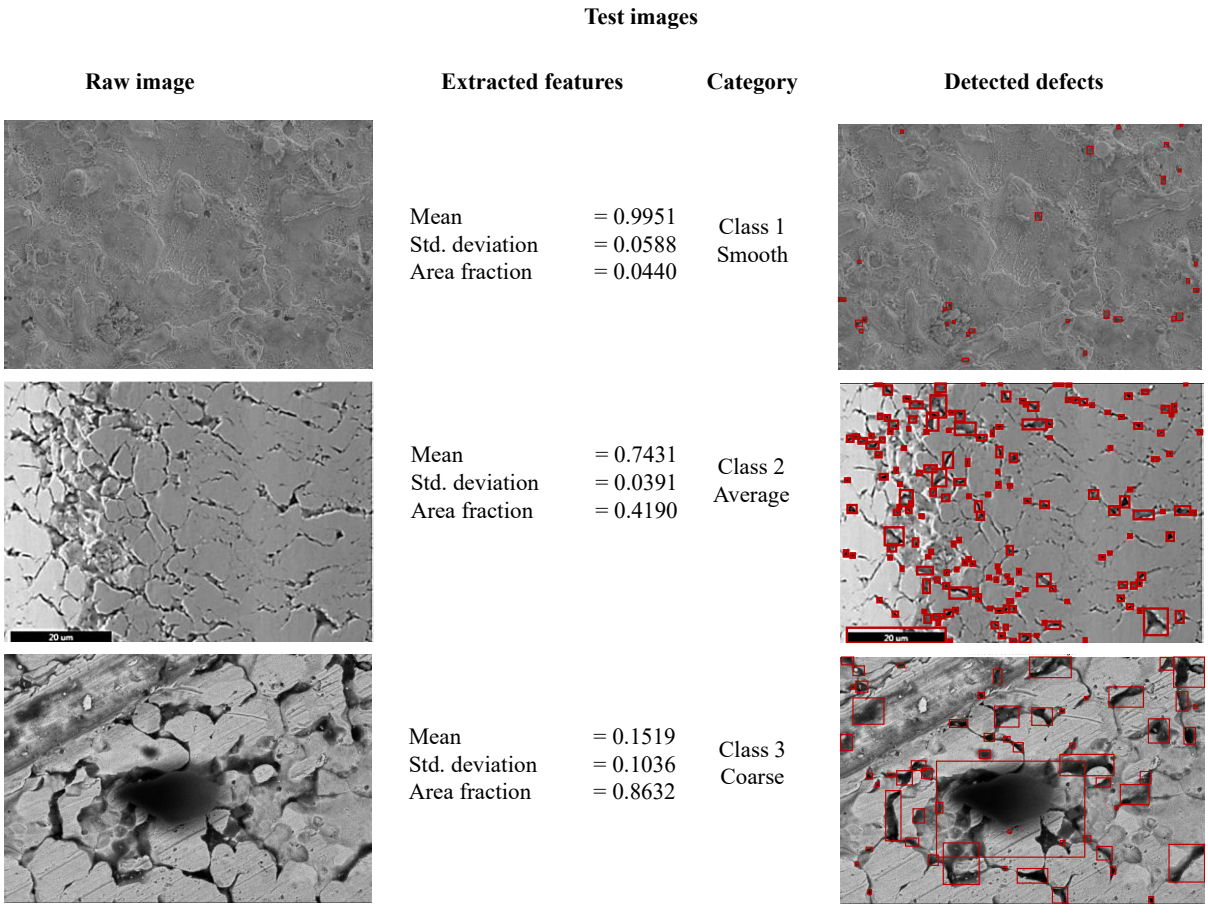

Fig. 15 Defect detection, feature extraction and surface classification for test images

4.1.1 Parameter suggestions

The algorithm suggests alternate parameter settings for machining if the image does not fall under smooth surface category. The micro defects during the finish pass are mostly due to lesser spark gap and lesser pulse off time for clearing the debris. Depending on how far the current test image datapoint is from the nearest class 1 datapoint, alternate suggestions are made. Nearness is based on the Euclidian distance considering mean, standard deviation, and defect fraction as the axes. A test datapoint (say, of an average category surface) closer to class 1 datapoint will need only a slight adjustment in parameter settings, whereas a test datapoint (of a coarse surface) far from class 1 datapoint will require more significant parameter changes.

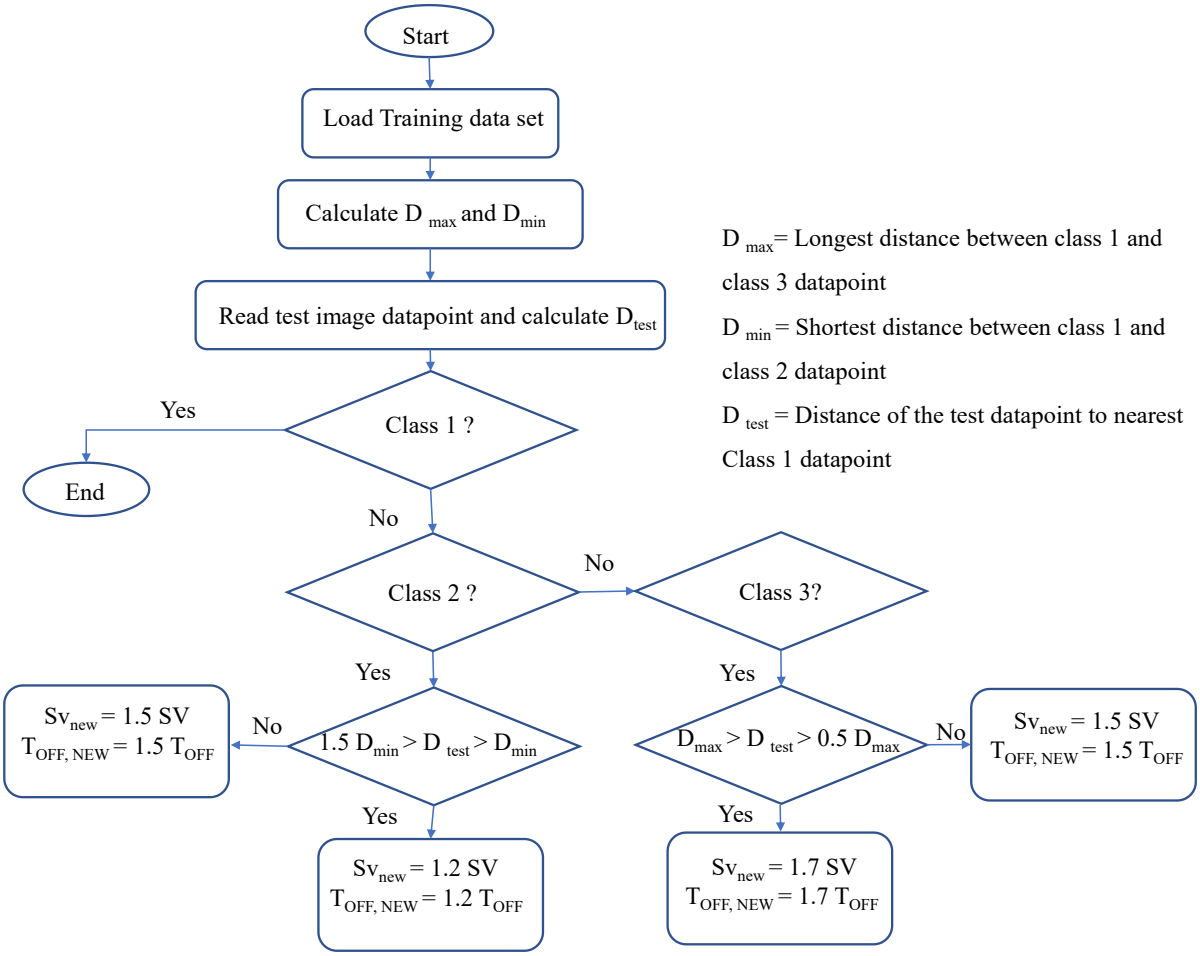

Fig. 16. Flowchart for parameter suggestion

Based on this logic, a feedback algorithm is developed to suggest alternate parameter settings if a test image falls in average or coarse category as shown in Fig. 17. The algorithm will recommend the user to increase pulse off time and servo voltage by various levels depending on the current micro defect level. By increasing the pulse off time and servo voltage the debris are more easily flushed off and the defects will reduce. If the distance of test datapoint is more from smooth category, greater changes are suggested in for pulse off time and servo voltage. Based on the suggested settings, the surface can be re-machined to obtain a better level of quality.

The input test image was machined with the following parameter settings: (T_{ON} = 8 µs, T_{OFF} =10 µs and SV=12 V). Based on the algorithm, the revised parameter settings are as follows

- Revised T_{ON} = T_{ON} = 8 µs
- Revised T_{OFF} = 1.7 T_{OFF} = 17 µs
- Revised SV= 1.7 SV = 20 V

This is represented in Fig. 18, where the alternate parametric settings are displayed. For the nine confirmation test experiments, the surface finish improvement by parameter revision is detailed in Table

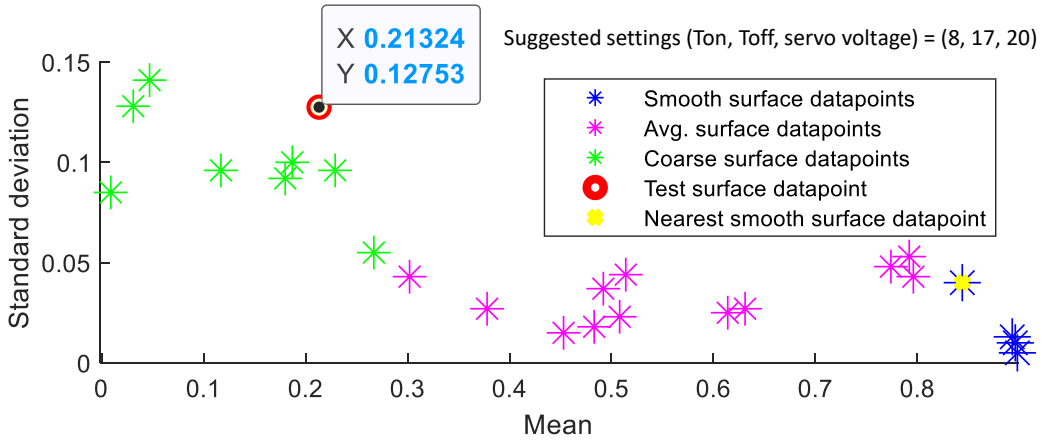

Fig. 17 Alternate parameter suggestions based on the nearest 'smooth' surface datapoint

Table 8 Comparison of surface finish under revised parameter settings

S. No.	T_{on} (μs)	T_{off} (μs)	SV (V)	Extracted features			Class	Revised class	R_a (μm)	Revised R_a (μm)
				Mean	Standard deviation	Defect area fraction				
1	6	12	24	0.893	0.013	0.118	1	-	0.81	-
2	5	18	21	0.884	0.016	0.137	1	-	0.85	-
3	11	19	17	0.673	0.043	0.341	2	1	2.43	0.98
4	14	11	16	0.217	0.121	0.861	3	1	3.51	0.84
5	15	12	15	0.013	0.085	0.989	3	1	3.23	0.77
6	17	10	15	0.161	0.065	0.784	3	1	3.77	0.87
7	15	19	22	0.472	0.027	0.482	2	1	2.44	0.94
8	13	18	25	0.511	0.038	0.531	2	1	2.06	0.62
9	12	20	21	0.688	0.029	0.419	2	1	2.16	0.71

As a future work, the authors plan to expand the training database, so that more parametric suggestions can be recommended to the user. Additionally, the performance of the proposed system to evaluate micro defects of the surfaces machined by different wire electric discharge machines can be performed.

5. Conclusions

The current study proposes algorithm for micro defect detection, quantification and classification of WEDM finish cut surfaces. Difficulties in conventional quantification of surface micro defects is highlighted and the solution is presented. The micro defect detection is based on digital image processing operations like histogram equalisation, binary conversion, gap filling and morphological operations. The algorithm is proved to be versatile in detecting linear, globular and porous defects. Based on the extracted features, input images are classified using the k-nearest neighbour algorithm. The developed system is a closed loop system which

classifies the WEDM finish cut surface, and based on the current defect level it can suggest alternate parameter settings to minimize the surface micro defects.

Acknowledgement

The authors would like to thank the central instrumentation facility (CIF), IIT Palakkad, for providing the test facility and equipment.

Declaration of Conflicting Interests

The Author(s) declare(s) that there is no conflict of interest.

Funding

The author(s) received no financial support for the research, authorship, and/or publication of this article.

References

1. Tyagi, A. (2019). Experimental and analytical investigations into wire electrochemical micro turning. Journal of Micromanufacturing, 2004; 2(1):42-58. https://doi.org/10.1177/2516598419827130
2. Bains, P. S., Mahajan, R., Sidhu, S. S., & Kaur, S. Experimental investigation of abrasive assisted hybrid EDM of Ti-6Al-4V. Journal of Micromanufacturing 2019; 2(2): 123–132. https://doi.org/10.1177/2516598419833498
3. Shandilya, P., Bisaria, H., & Jain, P. K. Parametric study on the recast layer during EDWC of a Ni-rich NiTi shape memory alloy. Journal of Micromanufacturing 2018; 1(2): 134–141. https://doi.org/10.1177/2516598418766934
4. Ho KH, Newman ST, Rahimifard S, et al. State of the art in wire electrical discharge machining (WEDM). Int J Mach Tools Manuf 2004; 44: 1247–1259.
5. Klocke F, Welling D, Klink A, et al. Evaluation of advanced Wire-EDM capabilities for the manufacture of fir tree slots in Inconel 718. Procedia CIRP 2014; 14: 430–435.

6. Goswami A, Kumar J. Trim cut machining and surface integrity analysis of Nimonic 80A alloy using wire cut EDM. Eng Sci Technol an Int J 2017; 20: 175–186.
7. Boban J, Ahmed A, Rahman MA, et al. Wire electrical discharge polishing of additive manufactured metallic components. Procedia CIRP 2020; 87: 321–326.
8. Abhilash PM, Chakradhar D. Surface integrity comparison of wire electric discharge machined Inconel 718 surfaces at different machining stabilities. Procedia CIRP 2020; 87: 228–233.
9. Li L, Wei XT, Guo YB, et al. Surface integrity of Inconel 718 by wire-EDM at different energy modes. J Mater Eng Perform 2014; 23: 3051–3057.
10. Li L, Guo YB, Wei XT, et al. Surface integrity characteristics in wire-EDM of inconel 718 at different discharge energy. Procedia CIRP 2013; 6: 220–225.
11. Yan MT, Lai YP. Surface quality improvement of wire-EDM using a fine-finish power supply. Int J Mach Tools Manuf 2007; 47: 1686–1694.
12. Abhilash, P. M., & Chakradhar, D. ANFIS modelling of mean gap voltage variation to predict wire breakages during wire EDM of Inconel 718. CIRP Journal of Manufacturing Science and Technology 2020; 31: 153–164. https://doi.org/10.1016/j.cirpj.2020.10.007
13. Abhilash, P. M., & Chakradhar, D. Surface integrity comparison of wire electric discharge machined Inconel 718 surfaces at different machining stabilities. Procedia CIRP 2020; 87: 228–233. https://doi.org/10.1016/j.procir.2020.02.037
14. Abhilash, P. M., & Chakradhar, D. Sustainability improvement of WEDM process by analysing and classifying wire rupture using kernel - based naive Bayes classifier. Journal of the Brazilian Society of Mechanical Sciences and Engineering 2021; 43(64) https://doi.org/10.1007/s40430-021-02805-z
15. Katz R, Srivatsan V, Patil L. Closed-loop machining cell for turbine blades. Int J Adv Manuf Technol 2011; 55: 869–881.

16. Quinsat Y, Dubreuil L, lartigue C. A novel approach for in-situ detection of machining defects. Int J Adv Manuf Technol 2017; 90: 1625–1638.
17. Chen S, Lin B, Han X, et al. Automated inspection of engineering ceramic grinding surface damage based on image recognition. Int J Adv Manuf Technol 2013; 66: 431–443.
18. Martínez SS, Vázquez CO, García JG, et al. Image fusion for surface finishing inspection. IST 2015 - 2015 IEEE Int Conf Imaging Syst Tech Proc 2015; 3–8.
19. Satorres Martínez S, Ortega Vázquez C, Gámez García J, et al. Quality inspection of machined metal parts using an image fusion technique. Meas J Int Meas Confed 2017; 111: 374–383.
20. Tsai DM, Rivera Molina DE. Morphology-based defect detection in machined surfaces with circular tool-mark patterns. Meas J Int Meas Confed 2019; 134: 209–217.
21. Steiner D, Katz R. Measurement techniques for the inspection of porosity flaws on machined surfaces. J Comput Inf Sci Eng 2007; 7: 85–94.
22. Świłło SJ, Perzyk M. Automatic inspection of surface defects in die castings after machining. Arch Foundry Eng 2011; 11: 231–236.
23. Świłło SJ, Perzyk M. Surface Casting Defects Inspection Using Vision System and Neural Network Techniques. Arch Foundry Eng 2013; 13: 103–106.
24. Liao Y, Weng X, Swonger CW, et al. Defect detection and classification of machined surfaces under multiple illuminant directions. Appl Digit Image Process XXXIII 2010; 7798: 77981T.
25. Huang DC, Lin CF, Chen CY, et al. The Internet technology for defect detection system with deep learning method in smart factory. 2018 4th Int Conf Inf Manag ICIM 2018 2018; 98–102.

26. Frayman Y, Zheng H, Nahavandi S. Machine Vision System for Automatic Inspection of Surface Defects in Aluminum Die Casting. J Adv Comput Intell Intel Informatics 2006; 10: 281–286.
27. Manish R, Venkatesh A, Denis Ashok S. Machine Vision Based Image Processing Techniques for Surface Finish and Defect Inspection in a Grinding Process. Mater Today Proc 2018; 5: 12792–12802.
28. Li W, Field KG, Morgan D. Automated defect analysis in electron microscopic images. npj Comput Mater 2018; 4: 1–9.
29. Reed RC. The Superalloys Fundamentals and Applications. Cambridge, 2006. Epub ahead of print 2006. DOI: 10.15713/ins.mmj.3.
30. Thakur DG, Ramamoorthy B, Vijayaraghavan L. Study on the machinability characteristics of superalloy Inconel 718 during high speed turning. Mater Des 2009; 30: 1718–1725.
31. Kumar V, Gupta P. Importance of Statistical Measures in Digital Image Processing. Int J Emerg Technol Adv Eng 2012; 2: 56–62.